

Brief Communication: Rapid $\sim 335 \text{ } 10^6 \text{ m}^3$ bed erosion after detachment of the Sedongpu Glacier (Tibet)

Andreas Kääb¹, Luc Girod¹

5 ¹Department of Geosciences, University of Oslo, Oslo, 0316, Norway

Correspondence to: Andreas Kääb (kaeaeab@geo.uio.no)

Abstract. Following the $130 \pm 5 \text{ } 10^6 \text{ m}^3$ detachment of the Sedongpu Glacier, south-eastern Tibet, in October 2018 the Sedongpu valley, which drains into the Yarlung Tsangpo (Brahmaputra) River, underwent rapid large-volume landscape changes. Between December 2018 and 2022 and in particular during summer 2021, an enormous volume of in total $\sim 335 \pm 5 \text{ } 10^6 \text{ m}^3$ was eroded from the former glacier bed, forming a new canyon of up to 300 m depth, 1 km width and almost 4 km length. The 2021 erosion peak happened through massive but still gradual retrogressive erosion into the former glacier bed. Several rock-ice avalanches of in total $\sim 150 \pm 5 \text{ } 10^6 \text{ m}^3$ added to the total rock, sediment and ice volume of over 0.6 km^3 that were exported from the basin since around 2017. The recent erosion volumes at Sedongpu are by order of magnitude equivalent to the average annual denudation volume of the entire ~~mountainous part of the~~ Brahmaputra ~~River~~ basin upstream of the location where the river leaves the Himalayas, and illustrate a potential and intensity for rapid post-glacial landscape evolution and the hazards related to such high-magnitude low-frequency events that have rarely been considered so far.

1 Introduction

Current retreat of mountain glaciers uncovers large areas of unconsolidated sediments that were previously held under ice and thus protected against most direct impacts by weather and climate. After glacier disappearance these areas are subject to 20 erosion processes at different time scales, from slow century-long background denudation to rapid mass loss by sediment-rich flows such as debris flows (Ballantyne, 2002; Carrivick and Heckmann, 2017; Williams and Koppes, 2019). Recent retreat of mountain glaciers is likely contributing to increased debris-flow activity and thus climate-change driven increase in mountain hazards (Zimmermann and Haeberli, 1992; Ballantyne, 2002; Hock et al., 2019). Glaciers retreat comparably slow, over many years to decades, so that the full potential erosion volume of formerly subglacial soft-beds is difficult to estimate 25 from the usual successive bed erosion that follows gradual glacier retreat. The reconstruction of original subglacial sediment volumes or eroded volumes, respectively, is difficult at the locations of former valley glaciers, unless significant parts of the glacier bed are still preserved.

Rare but massive glacier detachments offer a unique natural experiment to investigate what happens to a glacier bed once the glacier above it is rapidly removed, giving an indication of the maximum erosion potential that might else be mobilized over

30 longer time scales of gradual glacier retreat. During such large-volume detachments entire low-angle valley glaciers are removed within minutes (Kääb et al., 2018; Jacquemart et al., 2020; Kääb et al., 2021), leaving their beds suddenly exposed to weather and climate impacts. Low-angle glacier detachments seem to be associated with particularly soft, and thus easily erodible basal sediments (Gilbert et al., 2018; Kääb et al., 2021). A very recent and at the same time one of the largest glacier detachments known to date is the 2018 Sedongpu, Tibet, event. In this study, we investigate the development of the glacier bed after glacier removal in order to draw conclusions about bed stability and erosion potential, the landscape evolution in response to glacier loss, and the associated hazard potential. We summarize key site information and the 2018 glacier detachment, quantify the glacier-bed volume changes until ~~today (2022)~~ and other landscape changes in the basin, and discuss and conclude about our findings.

2 Study site

40 The Sedongpu glacier was situated in south-eastern Tibet (29.80° N, 94.92° E), at an elevation of about 3700 m asl., just 4 km north of the Yarlung Tsangpo River (Tibetan name for the upper reaches of Brahmaputra-River), which the Sedongpu valley joins at an elevation of around 2700 m asl. Highest point of the Sedongpu catchment is the Gyala Peri peak (7294 m asl.; Fig. 1). The study site, in particular the western flank of Gyala Peri represents extreme topography in terms of relief and overall slope angles. The Gyala Peri and neighbouring Namcha-Barwa massifs have exceptionally high uplift and denudation rates at million-year time scales (King et al., 2016), and the Yarlung Tsangpo an exceptionally high stream power, up to ~4000 W m⁻² in the Yarlung Tsangpo gorge into which the Sedongpu valley drains (Finnegan et al., 2008). At the Nyingchi meteorological station (c. 3000 m.asl., c. 50 km west of Sedongpu), the warmest months are July and August (mean daily maximum around 20 °C, mean daily minimum 13 °C), and the coldest month is January (mean daily maximum 4 °C, mean daily minimum –8 °C). Highest mean monthly precipitations at Nyingchi are around 115 mm/month in July and August, and 50 lowest in November and December with around 10 mm. Sedongpu glacier rested on an- elevated sediment/moraine bed (Haeberli et al., 2002) and the glacier surface had a c. 30-50 m higher elevation than the closest valley floor surrounding it. The study wider region shows the strongest glacier volume losses currently found in High-Mountain Asia (Hugonnet et al., 2021). According to Obu et al. (2019) the Sedongpu Glacier ~~should have been~~was several hundred metres in elevation below the regional permafrost limit.

55 3 Data and Methods

Here, we mainly generate and investigate optical stereo data acquired by the Pleiades and Spot 6/7 satellites. We use the MicMac software (Rupnik et al., 2016; Rupnik et al., 2017) to produce DEMs and orthoimages of 13 Nov 2015 (Spot 6 tri-stereo; before detachment), 30 Dec 2018 (Pleiades tri-stereo; two months after detachment), 12 Jan 2020 (Spot 7 stereo), 30 April 2021 (Pleiades tristereo), 19 Sep 2021 (Pleiades stereo), and 4 Nov 2022 (Spot 6 tristereo). All DEMs are generated

60 and co-registered using standard procedures. Elevation and volume changes between our repeat DEMs can be estimated in different DEM combinations that should then sum up to the same amount. From the associated triangulation (or loop) errors we obtain an average uncertainty for our volume estimates of around $\pm 1 \cdot 10^6 \text{ m}^3$. From stable ground areas we estimate a standard deviation of elevations of $\pm 4 \text{ m}$ and a standard error of mean elevation changes over the glacier and rock avalanche sites of around $\pm 1 \text{ m}$, translating to an uncertainty of around $\pm 5 \cdot 10^6 \text{ m}^3$ for the volume change estimates. We choose the latter
65 more conservative estimate as our volume change uncertainty.

4 The 2018 glacier detachment

In addition to a number of smaller mass flows from the catchment until 2017, two 17 and $33 \cdot 10^6 \text{ m}^3$, respectively, rock-ice avalanches from the Gyala Peri west flank ran over the Sedongpu glacier late in October 2017 (Kääb et al., 2021; Li et al., 2022). Following the 2017 rock-ice avalanche(s), the main Sedongpu Glacier underwent drastic changes. Ponds developed
70 on its surface and along the margins, surface velocities increased from a background velocity of $\sim 0.3 \text{ m day}^{-1}$ in 2017 to 25 m day^{-1} in mid-October 2018 (Kääb et al., 2021; Zhang et al., 2022) and the glacier surface showed increased crevassing. In two parts, on 16 Oct 2018 and 29 Oct 2018, the entire glacier tongue of in total $130 \pm 5 \cdot 10^6 \text{ m}^3$ detached, and additional
75 $\sim 44 \pm 5 \cdot 10^6 \text{ m}^3$ from surrounding moraines (Figs. 1-2, Supplementary Fig. S3), leaving the sediment previously beneath the Sedongpu Glacier entirely exposed. The mass temporary dammed up the Yarlung Tsangpo River, (Liu et al., 2019; Tong et al., 2019; Wang et al., 2020; Kääb et al., 2021; An et al., 2022; Zhang et al., 2022). The theoretical ice thickness estimates
80 for Sedongpu Glacier from Farinotti et al. (2019) agree on average well with the actual elevation loss between 2015 and December 2018 due to the glacier detachment, suggesting indicating that the $130 \cdot 10^6 \text{ m}^3$ glacier detachment volume might have consisted to a large extent of (though likely sediment-rich) ice rather than basal sediments. Pre-collapse ice-thickness datasets are however not of sufficient accuracy to evaluate whether the initial event was entirely composed of glacier ice,
85 whether it entrained basal sediment, and what the volume of sediment entrained might have been. This high ice content of the glacier detachment is confirmed by visual interpretation of the detachment zone and deposits in optical satellite data (Kääb et al., 2021). The ice thickness estimates by Millan et al. (2022) are roughly double and more of the above estimates and measurements, likely because they are based on 2017–2018 glacier surface velocities, which were in the case of Sedongpu Glacier already elevated increased due to pre-detachment surge-like acceleration (Kääb et al., 2021). This high ice content of the glacier detachment is confirmed by visual examination of the detachment zone and the deposits in post
85 collapse optical satellite data (Kääb et al., 2021) and the lack of a large erosional scar in the subglacial sediment, although we could not confirm this by direct field observations.

5 Rapid and massive bed erosion

The most prominent elevation change between 2015 and December 2018 is the glacier detachment from October 2018 (Figs. 90 2, Tab. 1, Supplementary Fig. S3) (Kääb et al., 2021). Maximum detachment depths over the glacier area were c. 200 m. The total elevation changes from Dec 2018 (i.e. after glacier detachment) until 2022 show a massive erosion pattern over much of the former glacier bed and its surrounding, amounting to about $335 \pm 5 \text{ } 10^6 \text{ m}^3$, 2.5 times the detached glacier volume, and with maximum erosion depths of 360 m and an average of 135 m over an area of 2.5 km^2 (Figs. 1-2, Tab. 1, [Supplementary Fig. S3](#)). Between Dec 2018 and 2020, erosion depths of up to 30–50 m can be found at limited areas along the deepest part 95 of glacier detachment area. The elevation changes January 2020 to April 2021 display a similar pattern. The April – September 2021 elevation changes contribute the by far largest part of the Dec 2018–2022 erosion of the glacier bed; $279 \pm 5 \text{ } 10^6 \text{ m}^3$ with a maximum depth of around 310 m. During September 2021 and November 2022 another around $32 \text{ } 10^6 \text{ m}^3$ were eroded from the area of the newly formed canyon.

To better understand the massive erosion amounts detected between the 30 April and 19 September 2021 DEMs, we 100 investigated optical and radar satellite data during this time period. Due to almost permanent cloud cover during this season over the study site only very few useful optical data (Planet, Sentinel-2, Landsat) are available, and the most dense information stems thus from Sentinel-1 radar data. Combined, these data show a steady increase of the erosion area and suggest thus that the massive erosion happened gradually, or at least in a series of relatively smaller events, mainly during 105 June–August and into early September 2021, rather than through one or a few massive landslides or debris flows. Between Dec 2018 (i.e. shortly after glacier detachment) and Apr 2021 the erosion was mainly concentrated along the drainage stream that developed through the detachment zone and corresponding avalanche path towards Yarlung Tsangpo (Fig. 2b, Suppl. Fig. S3). Suddenly in early June 2021, major erosion activity started at the point where the drainage stream left the former 110 glacier bed (star in Fig. 1b and c, Fig. 2b). From this point in time and space, massive but gradual up-valley retrogressive erosion formed the main canyon until end of Aug 2021 (see [Sentinel-1 images in Fig. 3 and the animation in the Supplement](#)). In fact, [state-of-the-art](#) early warning installations [including cameras and geophones at the outlet of the Sedongpu valley](#) registered rock-ice avalanches (following section) but no massive debris flows from the former glacier bed [and no river blockings of the Yarlung Tsangpo are reported](#) (Yang et al., 2023). [However, a new early warning station further up in the Sedongpu valley was only installed in May 2022, and then also able to detect debris flows from the catchment](#). Assuming gradual, temporally constant erosion activity over June–August 2021 gives an extreme sediment flux 115 of $3 \text{ } 10^6 \text{ m}^3$ every day over 3 months. [Another indication that supports the interpretation of gradual erosion is the fact that the fan of the Sedongpu valley in the Yarlung Tsangpo showed rapid changes during summer 2021 but seemed to have never dammed up the main river \(Sentinel-1 images in Fig. 3 and the animation in the Supplement\)](#) (Yang et al., 2023). Such [damming happened after the 2018 glacier detachment](#). In theory, the sediments eroded in summer 2021 could have had a very high ice content, or consisting of dirty ice, so that the mass could quickly loose volume due to melt. We find however 120 no indication of such ice in optical satellite data, and the glacier bed was likely temperate. The flanks of the erosion canyon

are very steep, at most places more than 30° and many places even 40° – 50° , suggesting the rapid summer 2021 erosion stopped for the time being at well-consolidated sediments.

6 Rock-ice avalanches and river erosion

Two other prominent landscape changes happened during 2018–2022 in the catchment. Further rock-ice volumes of in total

125 $100 \pm 5 \text{ } 10^6 \text{ m}^3$ were lost in the western flank of Gyala Peri, from the same area as the $50 \text{ } 10^6 \text{ m}^3$ rock-ice avalanche(s) of 2017, mentioned in Section 42. Of these roughly $100 \text{ } 10^6 \text{ m}^3$, $50 \text{ } 10^6 \text{ m}^3$ failed over Jan 2020–Apr 2021 (mostly on 22 March 2021; Bai et al. (2022); Zhao et al. (2022); Yang et al. (2023)) and another $50 \text{ } 10^6 \text{ m}^3$ during Apr 2021 – Nov 2022, all from the same area in the mountain flank (Fig. 1). These rock-ice avalanches are worth mentioning as their deposits will have contributed to the ice and sediment properties in the valley (Fig. 3f, Suppl. Fig. S3), and could also have directly affected the 130 ice and sediment stability there, for instance the Sedongpu Glacier detachment. Second, our DEMs include also a reach of around 6 km downstream of the location where the Sedongpu valley joins the Yarlung Tsangpo River. The fan of the Sedongpu valley shows a sequence of elevation gains and losses in response to the rock-ice mass flows from the Sedongpu valley, but there is no significant overall volume gain in the fan area and the ~6-km reach below (Fig. 2). This suggests that the river, having exceptionally high stream power (Section 2), was able to transport further most of the massive amount of 135 sediments that were deposited in particular during the 2018 glacier detachment and the June–September 2021 erosion peak. The Sentinel-1 image time series over summer 2021 (Fig. 3 and animation in the Supplement) shows rapid changes of the Sedongpu fan in extent, shape and height, but still these changes appear rather minor compared to the $279 \pm 5 \text{ } 10^6 \text{ m}^3$ erosion volume that should have entered the fan during this time period. It should be interesting to investigate in a further study, whether and where signs of deposition of such large volume can be observed along the Yarlung Tsangpo and Brahmaputra 140 River (Zhao et al. (2022) mention increased river turbidity 200 km downstream after the March 2021 rock-ice avalanche).

7 Discussion and conclusions

In sum, since 2017 and until November 2022 around $659 \pm 7 \text{ } 10^6 \text{ m}^3$ bedrock, sediment and ice debris have been exported from the Sedongpu catchment, most of it bedrock and sediments, and $335 \pm 5 \text{ } 10^6 \text{ m}^3$ of it eroded alone from the bed of the

145 former Sedongpu Glacier and its immediate surrounding. In the optical satellite images we find no indication of substantial amounts of massive ice in the latter volume (An et al., 2022). This extreme erosion amount corresponds to erosion rates of up to 30 m per month during June–August 2021 for the erosion area itself, locally up to 100 m per month (Tab. 1), or up to two metres per month if calculated as a mean for the entire basin area (total ca. 65 km^2 , c. 50 km^2 of it draining towards the Sedongpu Glacier). Such “ultra-rapid” rates of paraglacial landscape response (Meigs et al., 2006) are to our best knowledge 150 among the highest currently found on Earth.

An important question is to what extent general conclusions can be drawn from the extreme erosion volumes and rates that originate from the rapidly uncovered bed of Sedongpu Glacier. The subglacial material from below this glacier could be especially easily eroded. This would be in line with the assumption that large-volume detachments of low-angle valley glaciers seem to be associated with particularly soft glacier beds (Gilbert et al., 2018; Kääb et al., 2018; Kääb et al., 2021; Leinss et al., 2021). Precipitation data from the Sedongpu catchment are not available to us and could in such extreme topography substantially differ from the measurements at Nyingchi, 50 km to the west. At Nyingchi, during June–mid September 2021, 28 days with precipitation amounts > 10 mm are recorded, six of which with 40–70 mm. These total and daily amounts seem to be substantially higher compared to the same time period in other years (Supplementary Figs. S1 and S2). The massive 2021 erosion could thus have been triggered by exceptionally high precipitation amounts and rates. The main erosion activity, however, seems rather to have been a self-sustained, and perhaps self-enhancing, retrogressive destabilisation that, once triggered, formed the erosion canyon independent of precipitation amounts. This theory implies easily erodible, unconsolidated sediments, perhaps well water-saturated. The fact that the massive erosion activity in 2021 started exactly at the intersection of the former glacier boundary and the drainage stream (Sentinel-1 satellite images in Fig. 3 and animation in the Supplement) suggests that the former glacier bed was much more easily eroded than the surrounding moraines. Once a potential comparably stable protective surface layer on the former bed was incised through stream erosion, the underlying weak sediments could be mobilized. Alternatively, or additionally, enhanced stream erosion could have increased the terrain slope, or even undercut the former bed at the location of the erosion initiation. Such processes would not necessarily require any particularly high precipitation amounts and only be dependent on the time needed for the stream erosion to reach a (local) destabilisation threshold related to slope or spatial variation of sediment properties. Precipitation data at the Nyingchi station, ERA5 reanalysis data, and GPM IMERG satellite-derived precipitation data all suggest very little precipitation during the first half of August 2021. Still, Sentinel-1 radar data suggest continued massive erosion during that period (Supplement Fig. 3 and Supplementary animation). High precipitation amounts could have particularly saturated the sediments to make them prone to destabilisation, or could have contributed to accelerated stream incision or critical increase in local terrain gradients, though. Numerical modelling of the landscape evolution at Sedongpu could provide further constrains on the properties of the sediments and their mobilisation but is beyond the focus of this brief communication.

We have not systematically examined the erosion volumes after the other glacier detachments listed in Kääb et al. (2021). From visual interpretations of satellite imagery, though, we do not find equally extreme erosion in these other cases as found for Sedongpu, but note that some of the detachments are indeed associated with substantial post-detachment erosion activity (e.g., Flat Creek (Jacquemart et al., 2022), Amney Machen, Rasht valley/Petra Pervogo range). Another special circumstance involved in the extreme erosion in the Sedongpu valley, in addition to the potentially especially soft sediments, could be the elevated glacier bed where particularly large amounts of sediments were stored underneath the glacier, thus available to erosion. Sedimentary glacier beds are widespread in most glacierized mountains on Earth. Even if not fully understood, they are a sign of an imbalance in sediment flux where the production exceeds the export capacity from a glacier catchment

185 (Zemp et al., 2005) – not surprising for the comparably small Sedongpu catchment (total ca. 65 km², ca. 50 km² draining towards the glacier) that includes an enormous rock wall with substantial rock avalanche activity. Another open question is whether the erosion volumes at Sedongpu after rapid removal of the glacier are higher than they would be after gradual glacier retreat over decades and centuries. Some self-stabilizing effect could come into play over longer time intervals that does not act during rapid erosions, or vice-versa a self-enhancing process could act under such rapid erosions. At least over 190 decadal to centennial time-scales, the recent events at Sedongpu Glacier seem to represent a rapid and irreversible process of landscape transformation from a sediment-filled glacier valley to a glacier-free one with a deeply incised canyon.

The wider implications of the massive 2018–2022 erosion from the Sedongpu basin for mountain landscape development and sediment fluxes depend on the spatial and temporal reference scales considered, including the significance of the event in the magnitude-frequency distribution of mountain sediment transport. Even compared to rates of pro- and post-glacial 195 erosion that have so far been termed “ultra-rapid” (Meigs et al., 2006), the rates found in the Sedongpu valley since 2018 are exceptional. Compared to other glacier forefields, which typically show post-glacial erosion rates in the order of cm a⁻¹ (e.g., Delaney et al., 2018), the erosion volume at the former Sedongpu Glacier since 2018 is equivalent to several millennia of such average erosion rates. For entire glacier-hosting mountain ranges typical denudation rates are in the order of mm a⁻¹ (e.g., Islam et al., 1999; Hinderer et al., 2013; Thiede and Ehlers, 2013). Distributing the 2018–2022 Sedongpu erosion 200 volume to the entire area of the Brahmaputra catchment upstream of the location where the river leaves the Himalayan arch (Pasighat) gives 1–2 mm (depending on whether the rock avalanches are included or not). I.e., the recent Sedongpu erosion volume is by order of magnitude (compared to denudation rates from e.g. Islam et al., 1999; Thiede and Ehlers, 2013) equivalent to the annual denudation rate of a ~250,000 km² catchment. This implies that one or a few such events, in the present case triggered by glacier disappearance, can significantly vary the erosion rates of even one of the largest mountain 205 river catchments on Earth.

The events at Sedongpu confirm that glaciers are able to protect their soft beds against massive erosion. Once uncovered, the erosion potential of soft glacier beds is here demonstrated to be possibly enormous for some glaciers in terms of volumes and rates. Such erosion could be particularly extreme under the existence of fine-grained subglacial sediments, and – possibly combined – for elevated glacier beds where especially large amounts of subglacial sediments are stored. The 2018–2022 210 landscape development at Sedongpu represents an extreme example of rapid post-glacial slope response, a process that is indeed expected to be potentially particularly strong close to the time of glacier loss (Knight and Harrison, 2014). Lake outburst floods have been suggested to be major drivers of erosion in the Himalayas (Cook et al., 2018). The erosion volumes and rates at Sedongpu dwarf even those from lake outburst floods, though it is unclear how the frequency of both event types and thus their long-term volumes relate to each other. lake outburst floods, which have been suggested to be major drivers of erosion in the Himalayas (Cook et al., 2018). The changes at Sedongpu highlight an extreme glacier erosion potential and hazards related to it from debris flows and impacts on rivers. For instance, only the exceptionally large sediment transport capacity of the Yarlung Tsango let the river accommodate the extreme short-term erosion volumes delivered to it

without causing major river-damming. Such consequences of climate change in glacierized mountains have so far not been considered at this magnitude.

220 **Code availability**

The DEMs were generated using the open-source software MicMac (Rupnik et al., 2017; MicMac, 2022). The MicMac code used for the present study is available from Girod and Filhol (2022)

Data availability

225 Sentinel-1 and Sentinel-2 data are freely available from the ESA/EC Copernicus Sentinels Scientific Data Hub at <https://scihub.copernicus.eu> (Copernicus, 2020). Planet data (Dove and RapidEye) are not openly available as Planet is a commercial company. However, scientific access schemes to these data exist (<https://www.planet.com/markets/education-and-research/>). The original Pléiades and Spot stereo images are commercial (Airbus) and under academic license not transferable to other users. Several derived products can be made available on request for academic use as defined under the Airbus license.

230 **Author contribution**

A.K. developed the study concept, wrote the text, did most analyses and prepared the figures. L.G. prepared the DEMs, and commented to and edited the text.

Competing interests

All authors declare that they have no competing interests.

235 **Acknowledgements**

We thank the editor Harry Zekollari, referee Max Van Wyk de Vries, and another anonymous referee for their thoughtful and constructive comments. This study was conducted under ESA Glaciers_CCI and EarthExplorer 10 Harmony projects, and the University of Oslo “EarthFlows” research initiative.

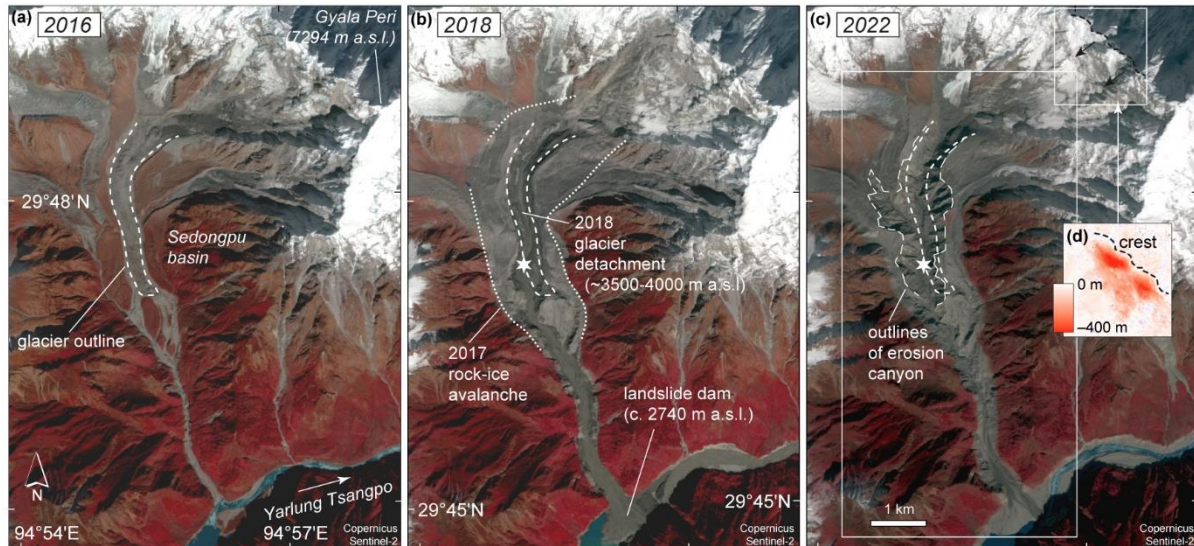
Financial support

240 This work was funded by the ESA project Glaciers_CCI (4000127593/19/I-NS), and the ESA EarthExplorer10 Mission Advisory Group (4000127656/19/NL/FF/gp).

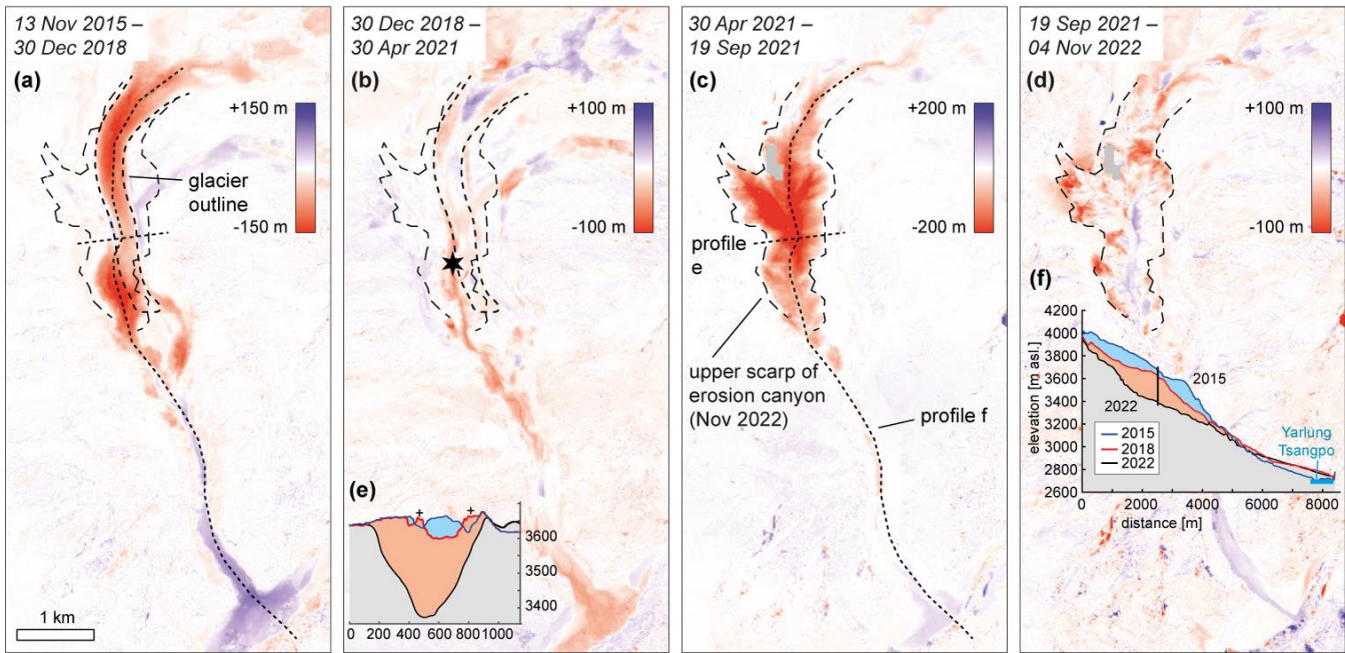
Table 1: Volume changes in the Sedongpu (Tibet) catchment over 2015–2022 as a consequence of glacier detachment, glacier bed erosion and rock-ice avalanches.

DEM data	Volume change glacier location (10^6 m^3 , M m^3 , \pm 5)	Maximum elevation change (m)	Average erosion rate (m a^{-1})	Comment	Volume change rock- avalanche site (10^6 m^3 , M m^3 , \pm 5)
13 Nov 2015	-174	-200		Oct 2018 glacier detachment, c. $130 \text{ } 10^6 \text{ m}^3$ from glacier, rest surrounding moraine	-50
30 Dec 2018	-12	-50	6		-1
12 Jan 2020	-12	-70	6	Contribution of rock-ice avalanche to changes at glacier location unclear	-50
30 Apr 2021	-279	-310	270	Erosion mostly in June–August 2021 (c. 30 m month^{-1})	-10
19 Sep 2021	-32	-120	10	Contribution of rock-ice avalanche to changes at glacier location unclear	-40
4 Nov 2022	-335	-360	30	Maximum depths not at same location	-101
12/2018- 11/2022	-508	-360	25	Average erosion rate from just before glacier detachment to 11/2022 c. 45 m a^{-1}	-151
11/2015- 11/2022					

245



250 | **Figure 1: Sedongpu basin on (a) 20 Nov 2016, (b) 31 Oct 2018, and (c) 19 Nov 2022 (credit: Copernicus Sentinel data). In 2017 a large rock-ice avalanche passed over the Sedongpu Glacier and in 2018, just before image (b) was taken, the glacier detached completely. Since then, a large $\sim 335 \text{ } 10^6 \text{ m}^3$ canyon eroded at the location of the former glacier bed with by far highest erosion rates during summer 2021. The location where the massive 2021 erosion started is marked by a star. Inset (d): Elevation changes 2015–2022 near the north crest of Gyala Peri showing the cumulative volume loss from three major $\sim 50 \text{ } 10^6 \text{ m}^3$ rock-ice avalanches. The small white rectangle indicates the position of the elevation change of inset (d). The large white rectangle indicates the location of Fig. 2.**



255 | **Figure 2: Elevation changes over four periods (a)–(d) as derived from DEMs from optical satellite stereo data (Pleiades and Spot 6/7, stereo and tri-stereo). Note, the value ranges of the elevation change legends vary between panels, depending on the magnitude of observed changes. Corresponding elevation change rates are given in Table 1. For the star in panel (b) see Fig. 1. Insets (e) and (f) are elevation profiles e and f of 13 Nov 2015, 30 Dec 2018 (after glacier detachment), and 4 Nov 2022. The + signs in inset (e) indicate 2015–2018 elevation increases from due to the 2017 rock-ice avalanche or splash deposits off from the 2018 glacier detachment. For profile locations see panels (a) and (c). A larger version of insets (e) and (f) can be found in the Supplement.**

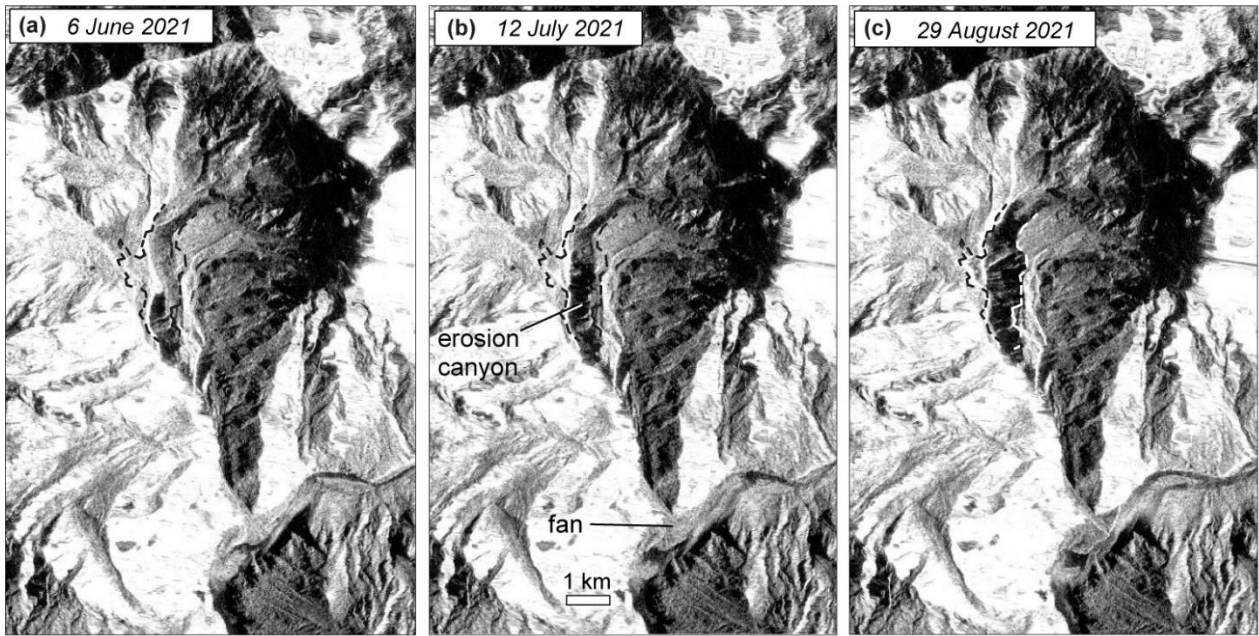


Figure 3: Ortho-rectified Sentinel-1 images over Sedongpu. The increasing dark area in the middle shows the evolution of the erosion canyon during summer 2021. Also note that the fan in the Yarlung Tsangpo is increasing in area. The lower-right margin of the fan appears bright in the image of 29.8.2021, indicating radar foreshortening and thus a steeper front towards the river. For a full series of Sentinel-1 images see the gif-animation in the Supplement.

References

270 An, B. S., Wang, W. C., Yang, W., Wu, G. J., Guo, Y. H., Zhu, H. F., Gao, Y., Bai, L., Zhang, F., Zeng, C., Wang, L., Zhou, J., Li, X., Li, J., Zhao, Z. J., Chen, Y. Y., Liu, J. S., Li, J. L., Wang, Z. Y., Chen, W. F., and Yao, T. D.: Process, mechanisms, and early warning of glacier collapse-induced river blocking disasters in the Yarlung Tsangpo Grand Canyon, southeastern Tibetan Plateau, *Sci Total Environ*, 816, Artn 151652, <https://doi.org/10.1016/j.scitotenv.2021.151652>, 2022.

275 Bai, L., Jiang, Y., and Mori, J.: Source processes associated with the 2021 glacier collapse in the Yarlung Tsangpo Grand Canyon, southeastern Tibetan Plateau, *Landslides*, 20, 421-426, <https://doi.org/10.1007/s10346-022-02002-6>, 2022.

Ballantyne, C. K.: Paraglacial geomorphology, *Quaternary Sci. Rev.*, 21, 1935-2017, [https://doi.org/10.1016/S0277-3791\(02\)00005-7](https://doi.org/10.1016/S0277-3791(02)00005-7), 2002.

Carrivick, J. L., and Heckmann, T.: Short-term geomorphological evolution of proglacial systems, *Geomorphology*, 287, 3-28, <https://doi.org/10.1016/j.geomorph.2017.01.037>, 2017.

280 Cook, K. L., Andermann, C., Gimbert, F., Adhikari, B. R., and Hovius, N.: Glacial lake outburst floods as drivers of fluvial erosion in the Himalaya, *Science*, 362, 53-57, <https://doi.org/10.1126/science.aat4981>, 2018.

Delaney, I., Bauder, A., Huss, M., and Weidmann, Y.: Proglacial erosion rates and processes in a glacierized catchment in the Swiss Alps, *Earth Surf Proc Land*, 43, 765-778, <https://doi.org/10.1002/esp.4239>, 2018.

285 Farinotti, D., Huss, M., Furst, J. J., Landmann, J., Machguth, H., Maussion, F., and Pandit, A.: A consensus estimate for the ice thickness distribution of all glaciers on Earth, *Nat Geosci*, 12, 168-173, <https://doi.org/10.1038/s41561-019-0300-3>, 2019.

Finnegan, N. J., Hallet, B., Montgomery, D. R., Zeitler, P. K., Stone, J. O., Anders, A. M., and Yuping, L.: Coupling of rock uplift and river incision in the Namche Barwa-Gyala Peri massif, Tibet, *Geol Soc Am Bull*, 120, 142-155, <https://doi.org/10.1130/B26224.1>, 2008.

290 Gilbert, A., Leinss, S., Kargel, J., Kääb, A., Gascoin, S., Leonard, G., Berthier, E., Karki, A., and Yao, T. D.: Mechanisms leading to the 2016 giant twin glacier collapses, Aru Range, Tibet, *Cryosphere*, 12, 2883-2900, <https://doi.org/10.5194/tc-12-2883-2018>, 2018.

Girod, L., and Filhol, S.: MicMac code. <https://zenodo.org/record/7380304#.ZBbbPt3MJPY>, 2022.

Haeberli, W., Kääb, A., Paul, F., Chiarle, M., Mortara, G., Mazza, A., and Richardson, S.: A surge-type movement at 295 Ghiacciaio del Belvedere and a developing slope instability in the east face of Monte Rosa, Macugnaga, Italian Alps, *Nor. J. Geogr.*, 56, 104-111, 2002.

Hinderer, M., Kastowski, M., Kamelger, A., Bartolini, C., and Schlunegger, F.: River loads and modern denudation of the Alps - A review, *Earth-Sci Rev*, 118, 11-44, <https://doi.org/10.1016/j.earscirev.2013.01.001>, 2013.

300 Hock, R., Rasul, G., Adler, C., Cáceres, B., Gruber, S., Hirabayashi, Y., Jackson, M., Kääb, A., Kang, S., Kutuzov, S., Milner, A., Molau, U., Morin, S., Orlove, B., and Steltzer, H.: High Mountain Areas, in: *IPCC Special Report on the Ocean and Cryosphere in a Changing Climate (SROCC)*, edited by: Pörtner, H.-O., Roberts, D. C., Masson-Delmotte, V., Zhai, P., Tignor, M., Poloczanska, E., Mintenbeck, E., Alegría, A., Nicolai, M., Okem, A., Petzold, J., Rama, B., and Weyer, N. M., Cambridge University Press, Cambridge UK and New York, USA 131-202, 2019.

305 Hugonnet, R., McNabb, R., Berthier, E., Menounos, B., Nuth, C., Girod, L., Farinotti, D., Huss, M., Dussaillant, I., Brun, F., and Kääb, A.: Accelerated global glacier mass loss in the early twenty-first century, *Nature*, 592, 726-731, <https://doi.org/10.1038/s41586-021-03436-z>, 2021.

Islam, M. R., Begum, S. F., Yamaguchi, Y., and Ogawa, K.: The Ganges and Brahmaputra rivers in Bangladesh: basin denudation and sedimentation, *Hydrol Process*, 13, 2907-2923, [https://doi.org/10.1002/\(SICI\)1099-1085\(19991215\)13:17<2907::Aid-Hyp906>3.0.Co;2-E](https://doi.org/10.1002/(SICI)1099-1085(19991215)13:17<2907::Aid-Hyp906>3.0.Co;2-E), 1999.

310 Jacquemart, M., Loso, M., Leopold, M., Welty, E., Berthier, E., Hansen, J. S. S., Sykes, J., and Tiampo, K.: What drives large-scale glacier detachments? Insights from Flat Creek glacier, St. Elias Mountains, Alaska, *Geol*, 48, 703-707, <https://doi.org/10.1130/g47211.1>, 2020.

Jacquemart, M., Welty, E., Leopold, M., Loso, M., Lajoie, L., and Tiampo, K.: Geomorphic and sedimentary signatures of 315 catastrophic glacier detachments: A first assessment from Flat Creek, Alaska, *Geomorphology*, 414, Artn 108376, <https://doi.org/10.1016/j.geomorph.2022.108376>, 2022.

King, G. E., Herman, F., and Guralnik, B.: Northward migration of the eastern Himalayan syntaxis revealed by OSL thermochronometry, *Science*, 353, 800-804, <https://doi.org/10.1126/science.aaf2637>, 2016.

Knight, J., and Harrison, S.: Mountain Glacial and Paraglacial Environments under Global Climate Change: Lessons from the Past, Future Directions and Policy Implications, *Geogr Ann A*, 96, 245-264, <https://doi.org/10.1111/geoa.12051>, 2014.

320 Kääb, A., Leinss, S., Gilbert, A., Buhler, Y., Gascoin, S., Evans, S. G., Bartelt, P., Berthier, E., Brun, F., Chao, W. A., Farinotti, D., Gimbert, F., Guo, W. Q., Huggel, C., Kargel, J. S., Leonard, G. J., Tian, L. D., Treichler, D., and Yao, T. D.: Massive collapse of two glaciers in western Tibet in 2016 after surge-like instability, *Nat Geosci*, 11, 114-120, <https://doi.org/10.1038/s41561-017-0039-7>, 2018.

Kääb, A., Jacquemart, M., Gilbert, A., Leinss, S., Girod, L., Huggel, C., Falaschi, D., Ugalde, F., Petrakov, D., Chernomorets, S., Dokukin, M., Paul, F., Gascoin, S., Berthier, E., and Kargel, J. S.: Sudden large-volume detachments of 325

low-angle mountain glaciers. More frequent than thought?, *Cryosphere*, 15, 1751-1785, <https://doi.org/10.5194/tc-15-1751-2021>, 2021.

Leinss, S., Bernardini, E., Jacquemart, M., and Dokukin, M.: Glacier detachments and rock-ice avalanches in the Petra Pervogo range, Tajikistan (1973-2019), *Nat Hazard Earth Sys*, 21, 1409-1429, <https://doi.org/10.5194/nhess-21-1409-2021>, 2021.

330 Li, W. L., Zhao, B., Xu, Q., Scaringi, G., Lu, H. Y., and Huang, R. Q.: More frequent glacier-rock avalanches in Sedongpu gully are blocking the Yarlung Zangbo River in eastern Tibet, *Landslides*, 19, 589-601, <https://doi.org/10.1007/s10346-021-01798-z>, 2022.

335 Liu, C. Z., Lu, J. T., Tong, L. Q., Chen, H. Q., Liu, Q. Q., Xiao, R. H., and Tu, J. N.: Research on glacial/rock fall-landslide-debris flows in Sedongpu basin along Yarlung Zangbo River in Tibet, *Geol. China*, 46, 219-234, 2019.

Meigs, A., Krugh, W. C., Davis, K., and Bank, G.: Ultra-rapid landscape response and sediment yield following glacier retreat, Icy Bay, southern Alaska, *Geomorphology*, 78, 207-221, <https://doi.org/10.1016/j.geomorph.2006.01.029>, 2006.

MicMac: <https://micmac.ensg.eu/index.php/Accueil>, 2022.

340 Millan, R., Mouginot, J., Rabaté, A., and Morlighem, M.: Ice velocity and thickness of the world's glaciers, *Nat Geosci*, 15, 124-129, <https://doi.org/10.1038/s41561-021-00885-z>, 2022.

345 Obu, J., Westermann, S., Bartsch, A., Berdnikov, N., Christiansen, H. H., Dashtseren, A., Delaloye, R., Elberling, B., Etzelmüller, B., Kholodov, A., Khomutov, A., Kääb, A., Leibman, M. O., Lewkowicz, A. G., Panda, S. K., Romanovsky, V., Way, R. G., Westergaard-Nielsen, A., Wu, T. H., Yamkhin, J., and Zou, D. F.: Northern Hemisphere permafrost map based on TTOP modelling for 2000-2016 at 1 km(2) scale, *Earth-Sci Rev*, 193, 299-316, <https://doi.org/10.1016/j.earscirev.2019.04.023>, 2019.

Rupnik, E., Deseilligny, M. P., Delorme, A., and Klinger, Y.: Refined satellite image orientation in the free open-source photogrammetric tools Apero/Micmac, *ISPRS Ann Photo Rem*, 3, 83-90, <https://doi.org/10.5194/isprsaanns-III-1-83-2016>, 2016.

350 Rupnik, E., Daakir, M., and Pierrot Deseilligny, M.: MicMac – a free, open-source solution for photogrammetry, *Open geospatial data, softw. stand.*, 2, 14, <https://doi.org/10.1186/s40965-017-0027-2>, 2017.

Thiede, R. C., and Ehlers, T. A.: Large spatial and temporal variations in Himalayan denudation, *Earth Planet Sc Lett*, 371, 278-293, <https://doi.org/10.1016/j.epsl.2013.03.004>, 2013.

355 Tong, L. Q., Tu, J. N., Pei, L. X., Guo, Z. C., Zheng, X. W., Fan, J. H., Zhong, X., Liu, C. L., Wang, S. S., He, P., and Chen, H.: Preliminary discussion of the frequent debris flow events in Sedongpu Basin at Gyala Peri peak, Yarlung Zangbo River, *J. Eng. Geol.*, 26, 1552-1561, <https://doi.org/10.13544/j.cnki.jeg.2018-401>, 2019.

Wang, W., Yang, J., and Wang, Y.: Dynamic processes of 2018 Sedongpu landslide in Namcha Barwa–Gyala Peri massif revealed by broadband seismic records, *Landslides*, 17, 409-418, <https://doi.org/10.1007/s10346-019-01315-3>, 2020.

Williams, H. B., and Koppes, M. N.: A comparison of glacial and paraglacial denudation responses to rapid glacial retreat, *Ann Glaciol*, 60, 151-164, <https://doi.org/10.1017/aog.2020.1>, 2019.

360 Yang, W., Wang, Z., An, B., Chen, Y., Zhao, C., Li, C., Wang, Y., Wang, W., Li, J., Wu, G., Bai, L., Zhang, F., and Yao, T.: Early warning system for ice collapses and river blockages in the Sedongpu Valley, southeastern Tibetan Plateau, *Nat. Hazards Earth Syst. Sci. Discuss*, [preprint] in review, <https://doi.org/10.5194/nhess-2023-38>, 2023.

Zemp, M., Kääb, A., Hoelzle, M., and Haeberli, W.: GIS-based modelling of glacial sediment balance, *Zeitschrift für Geomorphol. Suppl.*, 138, 113-129, 2005.

365 Zhang, X. P., Hu, K. H., Liu, S., Nie, Y., and Han, Y. Z.: Comprehensive interpretation of the Sedongpu glacier-related mass flows in the eastern Himalayan syntaxis, *J Mt Sci-Engl*, 19, 2469-2486, <https://doi.org/10.1007/s11629-022-7376-8>, 2022.

Zhao, C. X., Yang, W., Westoby, M., An, B. S., Wu, G. J., Wang, W. C., Wang, Z. Y., Wang, Y. J., and Dunning, S.: Brief communication: An approximately 50 Mm³ ice-rock avalanche on 22 March 2021 in the Sedongpu valley, southeastern Tibetan Plateau, *Cryosphere*, 16, 1333-1340, <https://doi.org/10.5194/tc-16-1333-2022>, 2022.

370 370 Zimmermann, M., and Haeberli, W.: Climatic change and debris flow activity in high-mountain areas - a case study in the Swiss Alps, *Catena Suppl.*, 22, 59-72, 1992.